Facile Conversion of Fe Nanotube Arrays to Novel α-Fe_2O_3 Nanoparticle Nanotube Arrays and Their Magnetic Properties

Xuelian Yu, Chuanbao Cao,* and Xiaoqiang An

Research Center of Materials Science, Beijing Institute of Technology, Beijing 100081, P. R. China

Received November 18, 2007. Revised Manuscript Received December 27, 2007

A simple template-based calcination treatment method has been developed to convert Fe nanotube arrays to novel α-Fe_2O_3 nanoparticle nanotube arrays (NPNTA). This process can conveniently be extended to fabricate a free-standing, easily oxidized metal oxide nanotube array, which may have future applications in nanoscale optics, electronics, and magnetics. The controlled variability of the diameter and length might be used to tune desired magnetic properties. The anisotropic magnetic property of both the discrepancy of the saturation magnetization (M_s) and coercivity (H_c) is observed for the NPNTA when the magnetic field is applied parallel and perpendicular to the nanoarrays. This remarkable magnetic anisotropy as well as the high H_c value makes these NPNTA can be useful for high-density magnetic recording applications.

1. Introduction

Recent studies on future high-density recording media have been focused on compounds which have high anisotropy and can be prepared with grains in the nanoscale size with coercivity (*Hc*) higher than 1000 Oe.[1] High magnetocrystalline anisotropy is needed to avoid thermal fluctuations and demagnetizing fields that tend to destabilize the magnetization of the recorded bits.[2] So more and more researches are focused on arrays of one-dimensional (1D) nanostructures through patterned perpendicular media.[3–5] The large aspect ratio of length/diameter of the 1D nanowire is thought to cause difficulty in recording with a narrow-gap inductive head since the recording field from that type of head localizes only the top of the particle.[6] To overcome this problem, magnetic particle one-dimensional array with perpendicular crystal anisotropy is one of the most promising candidates, since it has a potential to reach the extreme area density[7] of 1 Tbit/in.^{2}.

Among magnetic nanomaterials, α-Fe_2O_3 is the most stable iron oxide under ambient conditions and has n-type semiconducting, magnetic, nontoxic, and corrosion-resistant properties. So great efforts has been done on the synthesis of one-dimensional (1D) α-Fe_2O_3 nanostructures, including nanowires and nanotubes,[8–13] which are believed to possess peculiar properties due to the shape effect. However, the structure of nanoparticle nanotube arrays (NPNTA), which combine nanotube geometry with nanoparticle properties, and their magnetic property related to their unique structure have never been reported before.

Herein we demonstrate, for the first time, the facile calcinations method to transform Fe nanotube arrays to novel α-Fe_2O_3 nanoparticle nanotube arrays (NPNTA) under the help of PC template. As an improtant soft magnetic material, we are able to prepare high-quality Fe nanotube arrays with tunable magnetic properties by controlling the growth conditions. According to the unique NPNTA structure after calcination, it was believed these α-Fe_2O_3 might be useful in fabricating fillers and catalysts, etc.[14] Here we mainly discuss their anisotropic magnetic properties correlated with their small crystal size and porous appearance. Being single crystal particles at arrayed positions with high coercivity (1611 Oe) and perpendicular shape anisotropy, these NPNTA will have tremendous potential application as perpendicular recording media of high storage density.

2. Experimental Section

2.1. Preparation of Fe Nanotube Arrays. Commercially available polycarbonate membranes (Whatman Inc.) with cylindrical pores of diameter 0.05, 0.2, and 0.4 μm were used as templates in the electrochemical deposition. Before deposition, a thin (30 nm) layer of copper was sputtered on the bottom side of the membrane to connect to the graphite electrode, and it acted as the cathode.

* Corresponding author: e-mail cbcao@bit.edu.cn; Tel +86 10 6891 3792; Fax +86 10 6891 2001.

(1) Stavroyiannis, S.; Panagiotopoulos, I.; Niarchos, D. *Appl. Phys. Lett.* **1998**, *73*, 3453.
(2) Lambeth, D. N.; Velu, E. M. T.; Bellesis, G. H.; Lee, L. L.; Laughlin, D. E. *J. Appl. Phys.* **1996**, *79*, 4496.
(3) Morales, A. M.; Lieber, C. M. *Science* **1998**, *279*, 208.
(4) Che, G.; Fisher, E. R.; Martin, C. R. *Nature (London)* **1998**, *393*, 346.
(5) Shi, W. S.; Peng, H. Y.; Wang, N.; Li, C. P.; Xu, L.; Lee, C. S.; Kalish, R.; Lee, S. T. *J. Am. Chem. Soc.* **2001**, *123*, 11095.
(6) Haginoya, C.; Heike, S.; Ishibashi, M.; Nakamura, K.; Koike, K. *J. Appl. Phys.* **1999**, *85*, 8327.
(7) Sato, H.; Homma, T. *J. Nanosci. Nanotechnol.* **2007**, *7*, 225.
(8) Woo, K.; Lee, H. J.; Ahn, J. P.; Park, Y. S. *Adv. Mater.* **2003**, *15*, 1761.
(9) Xiong, Y. J.; Li, Z. Q.; Li, X. X.; Hu, B.; Xie, Y. *Inorg. Chem.* **2004**, *43*, 6540.
(10) Wang, R. M.; Chen, Y. F.; Fu, Y. Y.; Zhang, H.; Kisielowski, C. *J. Phys. Chem. B* **2005**, *109*, 12245.
(11) Wen, X. G.; Wang, S. H.; Ding, Y.; Wang, Z. L.; Yang, S. H. *J. Phys. Chem. B* **2005**, *109*, 215.
(12) Chen, J.; Xu, L.; Li, W. Y.; Gou, X. L. *Adv. Mater.* **2005**, *17*, 582.
(13) Jia, C. J.; Sun, L. D.; Yan, Z. G.; You, L. P.; Luo, F.; Han, X. D.; Pang, Y. C.; Zhang, Z.; Yan, C. H. *Angew. Chem., Int. Ed.* **2005**, *44*, 4328.
(14) Lahav, M.; Sehayek, T.; Vaskevich, A.; Rubinstein, I. *Angew. Chem., Int. Ed.* **2003**, *42*, 5576.

10.1021/cm703290s CCC: $40.75
Published on Web 02/01/2008

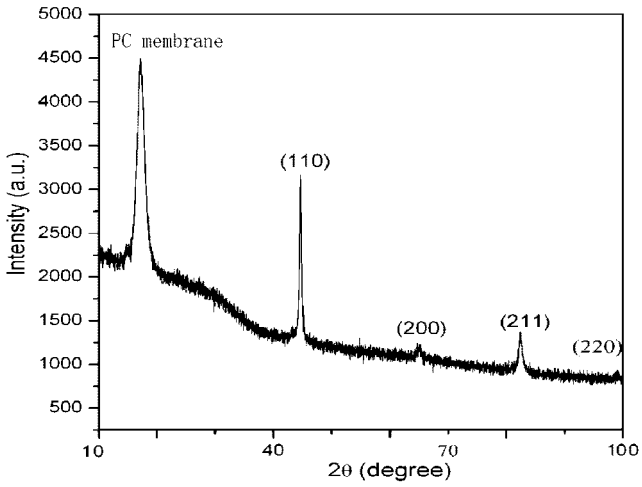

Figure 1. XRD pattern of Fe nanotube arrays embedded in the PC template.

The other graphite electrode acted as the anode in this two-electrode system. In the electrodeposition system all of the reactants used were of analytical grade. The electrolyte consisted of 0.05 M $FeSO_4 \cdot 7H_2O$, 0.05 M H_3BO_3, and deionized water. The deposition was carried out in constant-current mode; a typical deposition apparent current density was set to 1.5 mA/cm^2.

For SEM and TEM observation, the PC membrane templates were first dissolved into dichloromethane within few minutes and then carefully rinsed with deionized water several times, leaving behind the Fe nanotube which could be separated immediately using a magnet. The sample was then collected on a carbon-coated copper grid and allowed to air-dry before TEM measurement. For SEM observation, the obtained specimen was attached to an SEM stub using conductive paste.

2.2. Preparation of α-Fe_2O_3 Nanoparticle Nanotube Arrays (NPNTA). As the Fe nanotube arrays embedded in the PC membrane were obtained, they were put into a furnace for high-temperature oxidation in air. The sample was heated slowly to 800 °C and kept at this temperature for 2 h. The resulting samples were collected for the following experiments and characterization without any other process.

2.3. Characterization Techniques. The phase composition and structure of the as-synthesized products were examined by X-ray powder diffraction (XRD), operating on a Japan Rigaku Dmax RB X-ray diffractometer with Cu Kα radiation ($\lambda = 0.154\ 18$ nm). The morphology of the products was observed by scanning electron microscopy (SEM), using a JEOL-6700F scanning electron microanalyzer, and transmission electron microscopy (TEM), using a Hitachi H-800 transmission electron microscope with a tungsten filament and an accelerating voltage of 200 kV. Magnetic characterizations were performed by using the magnetic force microscopy (MFM, DI NS3a-MMAFM) and Lake Shore 7300 vibrating sample magnetometer (VSM) at room temperature. The magnetic anisotropic properties were investigated under fields applied parallel and perpendicular to the wire axis, respectively. To determine the curie transition temperature of α-Fe_2O_3 nanoparticle nanotube arrays, the temperature-dependent magnetization ($M-T$) curve was measured with 500 Oe magnetic field applied parallel to the arrays.

3. Results and Discussion

3.1. Fe Nanotube Arrays. Figure 1 presents the XRD pattern of the as-synthesized Fe nanotube arrays embedded in the PC membrane. All the diffraction peaks in the pattern can be indexed to the pure cubic phase iron, which are in good agreement with the literature value (JCPDS Card No. 06-0696). Miller indices of cubic-phase Fe were marked in this pattern.

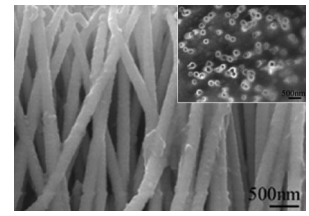

Figure 2. SEM images of the Fe nanotube arrays.

Figure 2 shows the SEM images of Fe nanotube arrays electrodeposited with 0.2 μm pore diameter polycarbonate membranes for plating time of 1 min. We can see the nanowires liberated from the PC template are well-aligned and uniform. These images show that the Fe nanotube arrays have the length of 5–6 μm, the diameter of 200 nm, which approximately correspond closely to the pore diameter and dimension of the PC membrane. The open ends (inset in Figure 2a) of the arrays further demonstrate the tubular structure of the resulting product.

To investigate the magnetic property related to their diameter, PC membranes with diameter 0.05 and 0.4 μm were used as template with the other experimental conditions the same. A preliminary study of the magnetic properties for fields applied parallel and perpendicular to the wire axis of Fe nanostructures (Figure 3) shows that all the Fe nanostructures exhibit enhanced coercivities (about 145–258 Oe) by comparison with that of the bulk Fe (∼1 Oe), with the easy magnetization axis being along the length of the wires for all the samples due to the shape anisotropy.[15] Furthermore, the coercivity of nanowire arrays is influenced by the diameter of the nanowires, and the values of coercivity (H_c) and squareness (S) with different diameters are listed in Table 1. It can be seen that reducing the diameter could improve the squareness and anisotropy of the magnetization hysteresis and raise the coercivity of nanotubes, which is in agreement with the results from the literature report on Ni nanowire arrays.[16] Hence, by controlling the growth conditions, we are able to prepare high-quality Fe nanotube arrays with desirable magnetic properties. These hollow soft magnetic nanotubes will open up possibilities for various new application fields, such as controlled-release capsules, artificial cells for drug delivery, lightweight fillers, shape-selective adsorbents, and catalysts.

In the next step, the Fe nanotube arrays embedded in PC membrane were put into a furnace for high-temperature calcination in air. The resulting samples were collected for the following characterization without any other process.

3.2. α-Fe_2O_3 Nanoparticle Nanotube Arrays (NPNTA). The phase and purity of the heat-treated product made from the slow oxidation of Fe nanotube arrays in PC membrane were determined from the XRD pattern (Figure 4). All of the diffraction peaks can be indexed to pure hexagonal

(15) Masuda, H.; Fukuda, K. *Science* **1995**, *268*, 1466.
(16) Nielsch, K.; Wehrspohn, R. B.; Barthel, J.; Kirschner, J.; Gosele, U. S.; Ficher, F.; Kronmuller, H. *Appl. Phys. Lett.* **2001**, *79*, 1360.

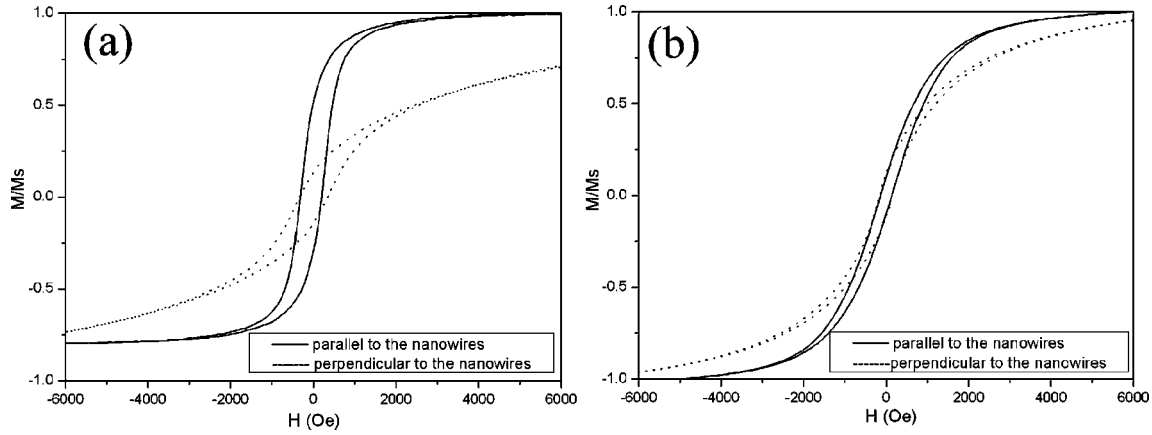

Figure 3. Hysteresis loop of Fe nanotube arrays with the diameter of (a) 50 nm and (b) 400 nm at room temperature.

Table 1. Comparison of Coercivity (H_c) and Squareness (S) with Different Diameters

	parallel to the wire		perpendicular to the wire	
diameter (nm)	H_c (Oe)	S	H_c (Oe)	S
50	258	0.45	345	0.19
200	94	0.317	145	0.16
400	139	0.10	149	0.12

α-Fe_2O_3 (JCPDF No. 33-0664). No characteristic peak was observed for other impurities such as Fe_3O_4 and γ-Fe_2O_3.

Figure 5 shows typical scanning electron microscopy (SEM) and transmission electron microscopy (TEM) images of the obtained α-Fe_2O_3 products with 0.2 μm pore diameter polycarbonate membranes after calcinations at different magnification. As can be seen (Figure 5a) that these arrays keep their packed pattern and scale after the removal of the PC template by annealing process. These images show that the α-Fe_2O_3 arrays have the length of 5–6 μm, the diameter of 200 nm, approximately, which correspond closely to the pore diameter and dimension of the PC membrane. The open ends (Figure 5b) of the arrays further demonstrate the hollow structure of the resulting product. The porous morphology of the walls is clearly demonstrated in Figure 5c, and the walls of the tubules are composed of coalesced nanoparticles (about 30 nm) shown in the inset in Figure 5c. Thus we can say the porous tubular nanostructures with rough walls composed of some nanoparticles, named nanoparticle nanotube arrays (NPNTA), are obtained. A transmission electron microscopy (TEM) image of an individual nanotube is shown in Figure 5d. There are pale and dark regions distributed along the tube, however, the particles are not clearly reflected because they are coalesced together in the wall. The related electron diffraction (ED) pattern indicates the single-crystalline nature of the nanoparticles forming the nanotube (inset in Figure 5d).

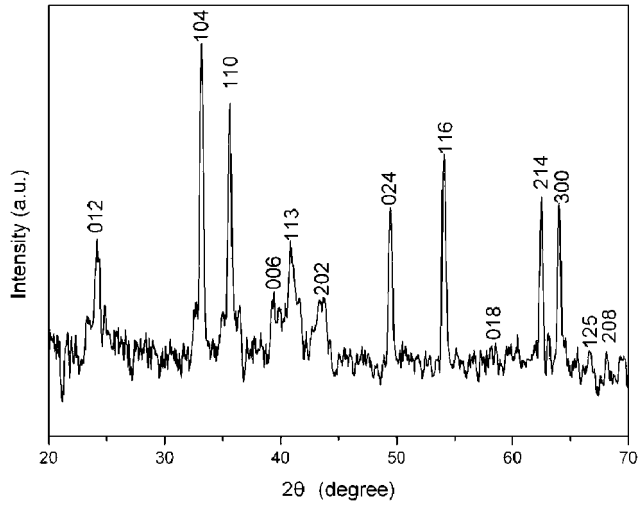

Figure 4. XRD pattern of α-Fe_2O_3 arrays after calcinations.

The transformation of the Fe nanotube arrays into porous α-Fe_2O_3 NPNTA and the preservation of the 1D morphology under calcinations are explained as follows: they are based on the crystal structure of Fe and the decomposition of PC template. Fe units are reserved in their original positions during calcinations to minimize the change in the Gibbs free energy for thermodynamic stability. This leads to the formation of Fe_2O_3 nanoparticles in the original Fe layers. Furthermore, during calcinations, water and gases from PC are generated and released, resulting in the formation of porous structure. This novel structure is expected to show properties combining nanoparticles and nantubes, such as high surface volume ratio, strong surface plasmon optical absorption and excellent catalysis, etc. In this paper we mainly discuss their magnetic property and their related potential application as perpendicular recording media of high storage density. To further investigate the magnetic property related to their diameter, PC membranes with diameter 0.05 and 0.4 μm were also used.

The magnetic properties of these nanoparticle nanotube arrays were probed using lift-mode magnetic force microscopy (MFM). Figure 6 shows the room temperature atomic force microscopy (AFM) and the corresponding magnetic force microscopy (MFM) images of the α-Fe_2O_3 NPNTA. The MFM image reflects the magnetic polarization of each nanoparticle nanotube arrays. The appearance of a dark and bright dot pattern in the MFM image corresponds to the top of each nanoparticles shown in the AFM image, suggesting that a spin domain is formed in the α-Fe_2O_3 NPNTA. The magnetic properties of the α-Fe_2O_3 NPNTA were further investigated using vibrating sample magnetometer (VSM).

Figure 7a shows the hysteresis loops at room temperature of the α-Fe_2O_3 NPNTA with the diameter of 50 nm measured by vibrating sample magnetometer measurements. The

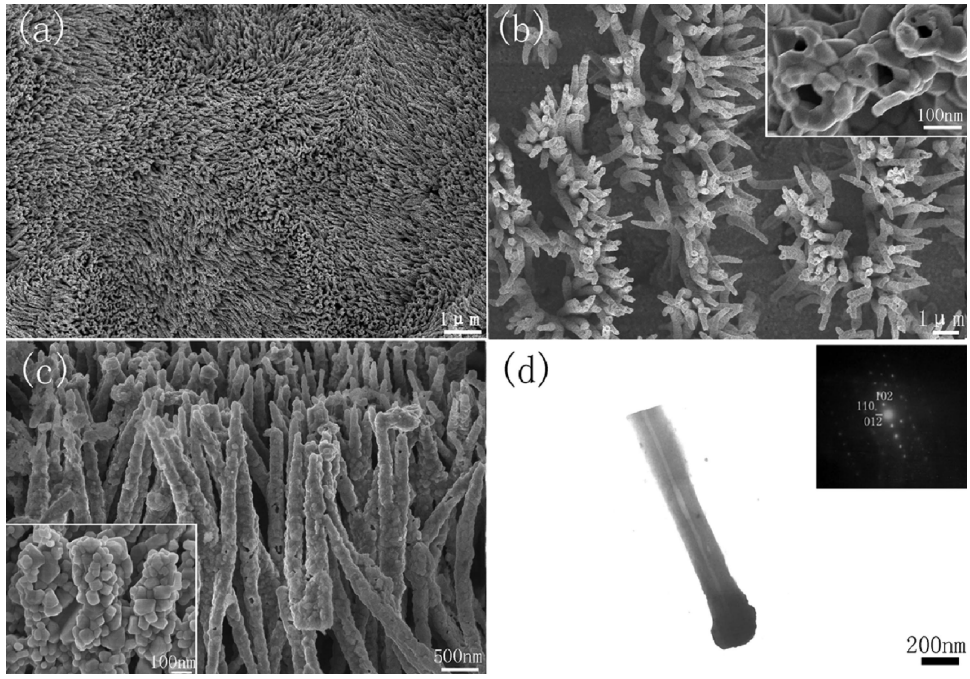

Figure 5. Typical SEM and TEM images of α-Fe_2O_3 NPNTA: (a) overall view; (b) top view; (c) side view; (d) TEM image of a single nanotube and corresponding ED pattern.

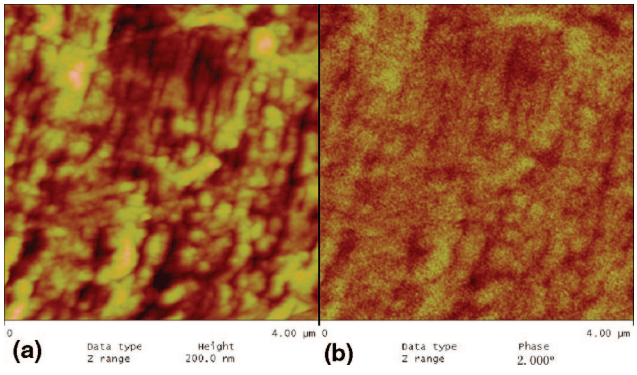

Figure 6. (a) AFM and (b) the corresponding MFM images of the α-Fe_2O_3 NPNTA with the diameter of 50 nm.

hysteresis loop of the nanostructure shows a ferromagnetic behavior with the coercivities (H_c) for an applied field parallel and perpendicular to the nanoarrays are about 1611.9 and 1442 Oe, respectively, at room temperature. This value is much higher than those of other morphologies of α-Fe_2O_3 nanomaterial, which are weak-ferromagnetic with the H_c about 200−300 Oe in room temperature.[17–20] Furthermore, we can see the coercivities (H_c) and the saturation magnetization (M_s) of the α-Fe_2O_3 NPNTA is dependent on the directions of the applied magnetic field. The easy magnetization axis is along the length of the arrays, demonstrating the anisotropic magnetization of the NPNTA.[21] Figure 7b displays the temperature dependent magnetization measured with 500 Oe magnetic field applied parallel to the arrays. Clearly, there is a Curie transition temperature T_c of 600 K, which is determined by the sharp peak in the dM/dT curve (inset in Figure 7b). Furthermore, the relationship of the coercivity with diameters of the nanotube arrays was also investigated. The values of coercivity (H_c) with different diameters are listed in Table 2. The high coercivity and anisotropic phenomena exist in all the three dimensions.

Although the source of high H_c and shape anisotropy of the α-Fe_2O_3 is not clear, the novel nanostructure might be a major reason. It is well-known that the magnetization of ferromagnetic materials is very sensitive to the morphology and structure of the as-synthesized sample.[22] So, since the well-grown α-Fe_2O_3 arrays are self-assembled using nanoparticles as building blocks, these nanoparticles are very close to each other, and some of them are in contact, the exchange and superexchange interactions between the surface atoms of neighboring nanoparticles are possible. The magnetic domains, for example, must overcome much higher energy barriers to align due to the interaction effect. Moreover, there exist sufficient spin interactions along the 1D nanotube shells due to the spatial confinement effect. Thus, the combining of nanotube geometry with nanoparticle properties leads to the origin of the unique magnetic properties. This remarkable magnetic anisotropy as well as the high H_c value needs further investigation. Nevertheless, there is no doubt that this NPNTA can be useful for high-density magnetic recording applications.

4. Conclusions

In summary, we have illustrated a facile strategy for converting metal nanotube arrays to its single-crystalline

(17) Chueh, Y. L.; Lai, M. W.; Liang, J. Q.; Chou, L. J.; Wang, Z. L. *Adv. Funct. Mater.* **2006**, *16*, 2243.
(18) Liu, L.; Kou, H. Z.; Mo, W. L.; Liu, H. J.; Wang, Y. Q. *J. Phys. Chem. B* **2006**, *110*, 15218.
(19) Wu, J. J.; Lee, Y. L.; Chiang, H. H.; Wong, D. K. *J. Phys. Chem. B* **2006**, *110*, 18108.
(20) Tang, B.; Wang, G. L.; Zhuo, L. H.; Ge, J. C.; Cui, L. J. *Inorg. Chem.* **2006**, *45*, 5196.
(21) Masuda, H.; Fukuda, K. *Science* **1995**, *268*, 1466.
(22) Sorescu, M.; Brand, R. A.; Tarabasanu, D. M.; Diamandescu, L. *J. Appl. Phys.* **1999**, *85*, 5546.

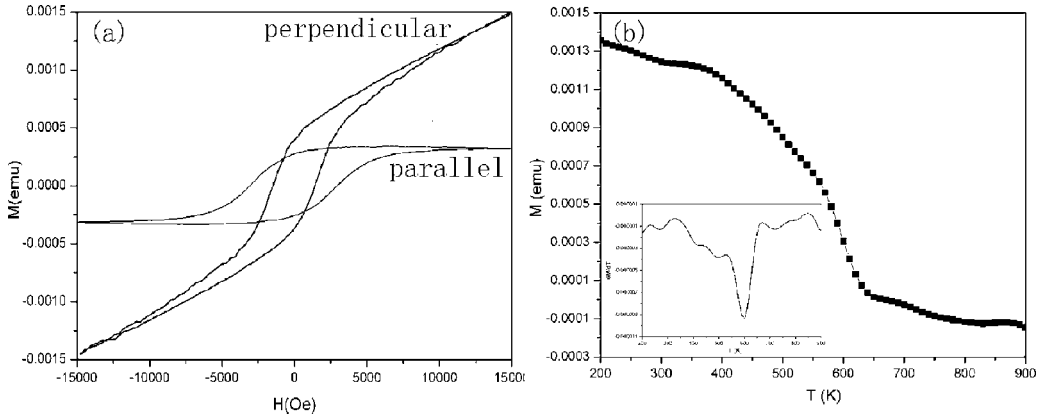

Figure 7. (a) Hysteresis loop at room temperature and (b) $M-T$ curve of α-Fe_2O_3 NPNTA.

Table 2. Comparison of Coercivity (H_c) with Different Diameters

diameter (nm)	H_c (Oe) (parallel to arrays)	H_c (Oe) (perpendicular to arrays)
50	1611.9	1442
200	1021	999
400	972	934

metal oxide nanotube arrays. The preservation of the morphology of individual nanotubes after the oxidation treatment suggests a promising route for fabricating parallel metal oxide nanotube arrays for future applications in nanosensors and other devices for optics or magnetics. Anisotropic magnetic property of both the discrepancy of the saturation magnetization (M_s) and coercivity (H_c) of α-Fe_2O_3 nanoparticle nanotube arrays is observed when the magnetic field is applied parallel and perpendicular to the nanoarrays. This remarkable magnetic anisotropy as well as the high H_c value makes these NPNTA attractive for high-density magnetic recording applications. If every ferromagnetic nanoparticles within the nanotube arrays acted as a recording unit, the magnetic recording density will be increased dramatically.

Acknowledgment. This work was supported by National Natural Science Foundation of China (Grants 20471007 and 10204003).

CM703290S